Plant Cell Rep (2017) 36:1083–1095
DOI 10.1007/s00299-017-2140-1

ORIGINAL ARTICLE

RRM domain of *Arabidopsis* splicing factor SF1 is important for pre-mRNA splicing of a specific set of genes

Keh Chien Lee[1] · Yun Hee Jang[1] · Soon-Kap Kim[2] · Hyo-Young Park[1] · May Phyo Thu[1] · Jeong Hwan Lee[3] · Jeong-Kook Kim[1]

Received: 22 February 2017 / Accepted: 4 April 2017 / Published online: 11 April 2017

Abstract

Key message **The RNA recognition motif of Arabidopsis splicing factor SF1 affects the alternative splicing of *FLOWERING LOCUS M* pre-mRNA and a heat shock transcription factor *HsfA2* pre-mRNA.**

Abstract Splicing factor 1 (SF1) plays a crucial role in 3′ splice site recognition by binding directly to the intron branch point. Although plant SF1 proteins possess an RNA recognition motif (RRM) domain that is absent in its fungal and metazoan counterparts, the role of the RRM domain in SF1 function has not been characterized. Here, we show that the RRM domain differentially affects the full function of the *Arabidopsis thaliana* AtSF1 protein under different experimental conditions. For example, the deletion of RRM domain influences AtSF1-mediated control of flowering time, but not the abscisic acid sensitivity response during seed germination. The alternative splicing of *FLOWERING LOCUS M* (*FLM*) pre-mRNA is involved in flowering time control. We found that the RRM domain of AtSF1 protein alters the production of alternatively spliced *FLM-β* transcripts. We also found that the RRM domain affects the alternative splicing of a heat shock transcription factor *HsfA2* pre-mRNA, thereby mediating the heat stress response. Taken together, our results suggest the importance of RRM domain for AtSF1-mediated alternative splicing of a subset of genes involved in the regulation of flowering and adaptation to heat stress.

Keywords Alternative splicing · *AtSF1* · *FLM* · Flowering time · Heat stress · RRM domain

Abbreviations

AP1	APETALA1
BBP	Branchpoint binding protein
CCA1	CIRCADIAN CLOCK ASSOCIATED1
LHY	LATE ELONGATED HYPOCOTYL
LFY	LEAFY
FLM	FLOWERING LOCUS M
FT	FLOWERING LOCUS T
Pre-mRNAs	PRECURSOR MESSENGER RNAS
RRM	RNA recognition motif
SF1	Splicing factor 1
SOC1	SUPPRESSOR OF OVEREXPRESSION OF CONSTANS1
SS	Splice site
SVP	SHORT VEGETATIVE PHASE
TOC1	TIMING OF CAB EXPRESSION1

Communicated by Jeong Sheop Shin.

Electronic supplementary material The online version of this article (doi:10.1007/s00299-017-2140-1) contains supplementary material, which is available to authorized users.

✉ Jeong Hwan Lee
jhwanlee90@jbnu.ac.kr

✉ Jeong-Kook Kim
jkkim@korea.ac.kr

[1] Division of Life Sciences, Korea University, 145 Anam-ro, Seongbuk-gu, Seoul 02841, Republic of Korea

[2] Center for Desert Agriculture, Division of Biological and Environmental Sciences and Engineering, King Abdullah University of Science and Technology, Thuwal 23955-6900, Saudi Arabia

[3] Department of Life Sciences, Chonbuk National University, 567 Baekje-daero, Deokjin-gu, Jeonju, Jeollabuk-do 54896, Republic of Korea

Introduction

Pre-mRNA splicing is an essential and tightly regulated process in eukaryotic systems. This process requires the removal of introns catalyzed by the spliceosome, consists of five major small nuclear ribonucleoproteins (U1, U2, U4, U5, and U6 snRNPs) and many more non-snRNP protein splicing factors (Jurica and Moore 2003). In mammalian systems, spliceosome assembly proceeds from the E′ complex to the C2 complex; in the spliceosomal E′ complex, U1 snRNP is recruited to the 5′ splice site (SS) and SF1/mBBP (also known as mammalian branchpoint binding protein) specifically recognizes the intron branch point sequence and interacts with the U2 snRNP auxiliary factor heterodimer (U2AF65 and U2AF35). Then, U2 snRNP binds to the polypyrimidine tract and 3′ SS, respectively, converting the E′ complex into the ATP-independent E′ complex (Chen and Manley 2009; Will and Luhrmann 2011).

The branchpoint binding protein (BBP) in yeast (*Saccharomyces cerevisiae*) and its mammalian ortholog SF1/mBBP is characterized by the presence of an N-terminal maxi-KH domain/KH-QUA-2 region, zinc knuckle (or zinc finger), and C-terminal proline-rich region (Arning et al. 1996; Abovich and Rosbash 1997). The maxi-KH domain of SF1/mBBP specifically recognizes and binds to branch point sequences (Liu et al. 2001), while the zinc knuckle domain has been implicated in RNA binding and raises the overall binding affinity (Berglund et al. 1997, 1998; Garrey et al. 2006). The domain architecture of these SF1 proteins is also largely conserved in plants (Lorkvic and Barta 2002; Wang and Brendel 2006; Schwartz et al. 2008), although plant SF1 proteins contain an addition RRM domain between the zinc finger and the proline-rich region when compared with their yeast and metazoan counterparts.

SF1 protein is important for viability in yeast (*S. cerevisiae*), roundworm (*Caenorhabditis elegans*), mice (*Mus musculus*), and human (Abovich and Rosbash 1997; Shitashige et al. 2007; Tanackovic and Krämer 2005). Depletion of SF1 from human cell lines or yeast compromises their viability and a knockout of *sf1* in mice was lethal. Moreover, the heterozygote $Sf1^{+/-}$ mouse has been used to show the effects of changes in the splicing pattern of certain pre-mRNAs (Shitashige et al. 2007). Recently, we identified a homolog of splicing factor SF1 that is essential for plant development in *Arabidopsis thaliana* (Jang et al. 2014). A homozygous T-DNA mutant of *AtSF1*, *atsf1-2*, had several developmental defects including early flowering, dwarfism, and abscisic acid (ABA) hypersensitivity. Moreover, we have shown that AtSF1 is involved in the alternative splicing of pre-mRNA of some genes. These results suggest that *AtSF1* is not essential for viability in *Arabidopsis*, unlike its yeast and metazoan counterparts.

Pre-mRNA splicing requires a large number of RNA binding proteins that possess one or two RNA recognition motifs (RRMs) (Alba and Pages 1998; Lorkovic et al. 2000; Lorkvic and Barta 2002). RRMs with approximately 80–90 amino acids form a four-stranded β-sheet packed against two α-helices (Birney et al. 1993; Maris et al. 2005). The most conserved sequences of the RRM, which are located in β1 and β3, consist of eight and six amino acids, named RNP1 and RNP2, respectively; these sequences are crucial for RNA binding (Bentley and Keene 1991; Birney et al. 1993). In *Arabidopsis*, 196 of RRM containing proteins have previously been identified through in silico searching for the RRM motif (Lorkvic and Barta 2002). There are some reports that the RRM domain is involved in RNA binding; protein–protein interactions; and protein targeting implicated in all aspects of RNA metabolism including pre-mRNA splicing, polyadenylation, mRNA transport, mRNA stability, and translation (Adam et al. 1986; Sachs et al. 1986; Glisovic et al. 2008; Lorkovic 2009; Tao et al. 2013).

In human SF1 and its yeast counterpart MSL5, the KH-QUA2 region is necessary and sufficient for the recognition of their branch point sequences in vitro (Liu et al. 2001; Jacewicz et al. 2015). Therefore, zinc fingers and other domains are presumably not necessary for branch point recognition in vivo. However, the other domains could have roles in other functions such as nuclear retention in yeast MSL5 (Rutz and Séraphin 2000). The aim of this study was to investigate the role of the RRM domain unique to plant SF1 proteins. As the RRM domain of plant SF1 proteins is well conserved in the plant kingdom, characterization of its function will provide us with useful information on plant splicing mechanisms.

Here, we investigated the role of the RRM domain in AtSF1 by expressing *AtSF1* lacking the RRM domain or with a deletion of the RNP1/2 motif under its own promoter in the *atsf1-2* mutant line ($pAtSF1_{2.4kb}$::*AtSF1ΔRRM:GUS atsf1-2*; $pAtSF1_{964bp}$::*AtSF1Δ RNP1/2:GUS*). We showed that the RRM domain of AtSF1 was necessary for the full restoration of *atsf1-2* mutant phenotypes such as early flowering, dwarfism, and heat stress tolerance. Furthermore, the restored flowering phenotype and heat stress response in $pAtSF1_{2.4kb}$::*AtSF1ΔRRM:GUS atsf1-2* plants correlated with changes in flowering time and heat stress-related genes, respectively. Our results suggest that the RRM domain of AtSF1 is involved in pre-mRNA splicing of genes involved in flowering time control and heat stress responses.

Materials and methods

Plant materials and growth conditions

Wild-type or transgenic *Arabidopsis* plants [ecotype Columbia (Col-0)] were grown in Sunshine Mix 5 (Sun Gro Horticulture, Agawarm, MA, USA) or Murashige and Skoog (MS) medium at 23 °C under LD conditions (16:8 h light:dark photoperiod) at a light intensity of 120 µmol m^{-2} s^{-1}. *atsf1-2* mutants (Jang et al. 2014) were used for plant transformation.

For heat treatments, 1-week-old *Arabidopsis* seedlings grown on MS plates were covered with aluminum foil to expose the plants to homogeneous heat conditions in darkness. The plates were transferred to a heat chamber set at 45 °C and incubated for 70 min. After heat treatments, the seedlings recovered at 23 °C for 3 days with white light illumination (Lee et al. 2015).

For ABA treatments, seeds were plated on medium containing 1% sucrose. At least 50 seeds per genotype were stratified at 4 °C for 3 days, and the seedlings with green cotyledons were scored after incubation for 6 days at 23 °C (Fujii et al. 2009).

Plasmid construction

To generate the *pAtSF1*$_{2.4kb}$*::AtSF1ΔRRM:GUS* and *pAtSF1*$_{2.4kb}$*::AtSF1:GUS* constructs, the coding sequences of *AtSF1* with or without the RRM domain were amplified using specific primers and cloned into the pBI101 vector. An *AtSF1* construct without RNPs (*pAtSF1*$_{964bp}$*::AtSF1ΔRRM:GUS*) was also generated using the same approach. To make the *35S::AtSF1ΔRRM:GUS* and *35S::AtSF1:GUS* constructs, amplified *AtSF1* coding sequences with or without the RRM domain were cloned into pBA-Myc vectors harboring the *35S* promoter. To produce constructs containing the full-length sequence of AtU2AF65a or AtU2AF65b containing only two RRM domains (RRM2/RRM3), the amplified coding sequences were cloned into the pGEX-5X-1 vector (GE Healthcare, Chicago, USA). The resulting recombinant plasmid was sequenced to verify the absence of PCR errors during amplification. Oligonucleotide sequences used in this study are listed in Supplementary Table S1.

Generation of transgenic plants and measurement of flowering time and leaf area

Transgenic plants were generated using the floral dip method with minor modifications (Weigel and Glazebrook 2006). *Agrobacterium tumefaciens* strain GV3101 harboring the gene constructs was infiltrated into the *atsf1-2* mutant background that showed silencing of *NPTII* gene for kanamycin resistance. Transgenic seedlings were first selected using kanamycin for pBI101 vector or BASTA for pBA-Myc vector and then verified by PCR-based genotyping. At least 20–30 T_1 seedlings were analyzed for each construct.

To score flowering time, the total numbers of rosette and cauline leaves of at least five or six independent transgenic lines (at least 16 individual plants per independent transgenic line) were counted in the T_2 or T_3 generation. To determine whether the flowering time of the transgenic plants differed significantly compared with the *atsf1-2* mutants, the data were analyzed using the SPSS software version 12.0 (IBM SPSS Statistics).

To measure leaf area, the rosette leaf area of at least 16 independent transgenic lines was analyzed using the ImageJ software.

Expression analysis

For RNA expression analysis, total RNA was extracted from whole seedlings using a Trizol reagent (Invitrogen, Carlsbad, CA, USA). Samples for RT-PCR or qRT-PCR were harvested at Zeitgeber time 16, unless stated otherwise, and were frozen immediately in liquid nitrogen before being stored at −80 °C until use. RNA quality was determined with a Nanodrop ND-2000 spectrophotometer (Nanodrop Technologies), and only high-quality RNA samples ($A_{260}/A_{230} > 2.0$ and $A_{260}/A_{280} > 1.8$) were used for subsequent experiments. cDNA synthesis was conducted according to the manufacturer's instructions and 1 µg of RNA was used (Roche Applied Science, Madison, WI, USA). The RT-PCR analysis was performed as described previously (Jang et al. 2014). The qRT-PCR analysis was carried out in 384-well plates with a LightCycler 480 (Roche Applied Science) using Roche SYBR Green Master mixture (Roche Applied Science). One stably expressed gene (*PP2AA3*) was used as a reference gene. All qRT-PCR experiments were carried out in three biological replicates (independently harvested samples) with three technical replicates each. For determination of relative abundance of transcripts, the detailed procedures were previously described (Lee et al. 2013). Oligonucleotide sequences used in this study are listed in Supplementary Table S1.

For protein expression analysis, whole seedlings were ground to a powder in liquid nitrogen and the powder was suspended in a buffered solution of 50 mM Tris–HCl (pH 8.0), 150 mM NaCl, 10% glycerol, 0.5% Triton X-100, 2 mM phenylmethanesulfonyl fluoride, and complete protease inhibitor cocktail (Roche Applied Science). The protein concentration was determined using Bradford solution (Bio-Rad, Hercules, CA, USA). Subsequently, proteins were separated using 10% SDS-PAGE, transferred onto PVDF membrane (Bio-Rad), as described previously (Kim et al. 2008). PVDF membranes were then probed with mouse monoclonal c-Myc antibody (9E10) diluted to 1:500 (Santa Cruz Biotechnology, Dallas, TX, USA) and subsequently incubated with secondary antibody diluted to 1:2000 (Enzo Life Sciences, UK). The membrane was treated using ECL detection reagent (Innotech, Daejon, Republic of Korea).

For GUS histochemical analysis, the procedure was performed as described by Chen et al. (1998).

In vitro pull-down analysis

In vitro pull-down analyses were conducted as described previously by Jang et al. (2014). Briefly, glutathione *S*-transferase (GST) fusion recombinant proteins were mixed with in vitro translation products synthesized using the T7 TNT-coupled Transcription/Translation System (Promega, Madison, WI, USA) and the mixtures were gently rotated for 2 h at 4 °C. Subsequently, they were washed three times with the washing buffer and eluted with 10 mM reduced glutathione in 100 mM NaCl and 20 mM Tris–HCl (pH 7.2). Finally, the eluted protein samples were analyzed by 12.5% SDS-PAGE and visualized by autoradiography.

Results

Deletion of the RRM domain from AtSF1 does not affect the stability of AtSF1 or its interaction with AtU2AF65 proteins

To determine whether the RRM domain of AtSF1 is important for AtSF1 activity, we generated transgenic plants overexpressing *AtSF1* lacking the RRM domain and fused to a 6x-Myc tag at the N-terminal region in the *atsf1-2* mutant background (*35S::cMyc:AtSF1ΔRRM atsf1-2*) (Fig. 1a). As the deletion of a large portion such as the RRM domain may result in mRNA instability or degradation of the truncated protein because of changes in its conformation (Severing et al. 2012), we first analyzed RNA and protein expression of the transgene in *35S::cMyc:AtSF1ΔRRM atsf1-2* plants. RT-PCR analysis showed that the full or truncated transgene was normally expressed in *35S::cMyc:AtSF1ΔRRM atsf1-2* and *35S::cMyc:AtSF1 atsf1-2* plants (Fig. S1). Western blot analysis confirmed that the overexpression of truncated or full AtSF1 proteins was also successfully detected in these plants (Fig. 1b), indicating that deletion of the RRM domain from AtSF1 does not affect the RNA or protein expression of the introduced transgene. However, the band intensity of AtSF1 signals was weaker in *35S::cMyc:AtSF1ΔRRM atsf1-2* plants than in *35S::cMyc:AtSF1 atsf1-2* plants, suggesting that the RRM domain may affect the protein stability of AtSF1 proteins.

The N-terminal ULM motif of SF1 is known to interact with the UHM (RRM3) domain of U2AF65 proteins (Selenko et al. 2003; Webb et al. 2005). Although we expected that truncated AtSF1 lacking the RRM domain would still interact with AtU2AF65, we examined their interaction to exclude the possibility that the truncated form of AtSF1 affected the interaction with AtU2AF65. *In vitro* pull-down assays revealed that truncated AtSF1 lacking the RRM domain still interacted with AtU2AF65a and AtU2AF65b to a similar extent as complete AtSF1 (Fig. 1c). This result indicates that the binding affinity of full or truncated AtSF1 to AtU2AF65 proteins is similar.

Taken together, these results suggest that truncated AtSF1 lacking the RRM domain could be functional in transgenic plants.

Expression of *AtSF1* lacking its RRM domain only partially rescues the effects of the *atsf1* mutation on flowering time and dwarfism

Previously, we have shown that a mutation in *AtSF1* results in pleiotropic developmental defects including slightly early flowering and dwarfism under normal growth conditions (Jang et al. 2014). To examine whether the RRM domain of AtSF1 is needed to rescue these developmental defects observed in *atsf1-2* mutants, we analyzed T_3 *35S::cMyc:AtSF1ΔRRM atsf1-2* plants. As shown in Fig. S2A and Supplementary Table S2, five independent *35S::cMyc:AtSF1ΔRRM atsf1-2* plants flowered with approximately 12 leaves under long-day (LD) conditions at 23 °C, indicating that the overexpression of *AtSF1ΔRRM* partially rescued the early flowering phenotype of the *atsf1* mutant. Conversely, five independent *35S::cMyc:AtSF1 atsf1-2* plants flowered with approximately 14 leaves. Thus, the flowering of *35S::cMyc:AtSF1 atsf1-2* plants was more similar to that of wild-type plants. Furthermore, both *35S::cMyc:AtSF1ΔRRM atsf1-2* and *35S:c:Myc:AtSF1 atsf1-2* plants had normal plant size and inflorescence phyllotaxy, similar to wild-type plants (Fig. S2B and C). These results indicate that the introduction of *35S::cMyc:AtSF1ΔRRM* partially rescues the flowering defects of *atsf1-2* mutants.

As the ectopic expression of *AtSF1ΔRRM* under the control of the *35S* promoter may cause potential side effects, we introduced the *AtSF1* construct lacking the RRM domain expressed under its own 2.4 kb promoter (*pAtSF1*$_{2.4kb}$*::AtSF1ΔRRM:GUS*) into *atsf1-2* mutants (Fig. 2a) and analyzed five independent *pAtSF1*$_{2.4kb}$*::AtSF1ΔRRM:GUS*

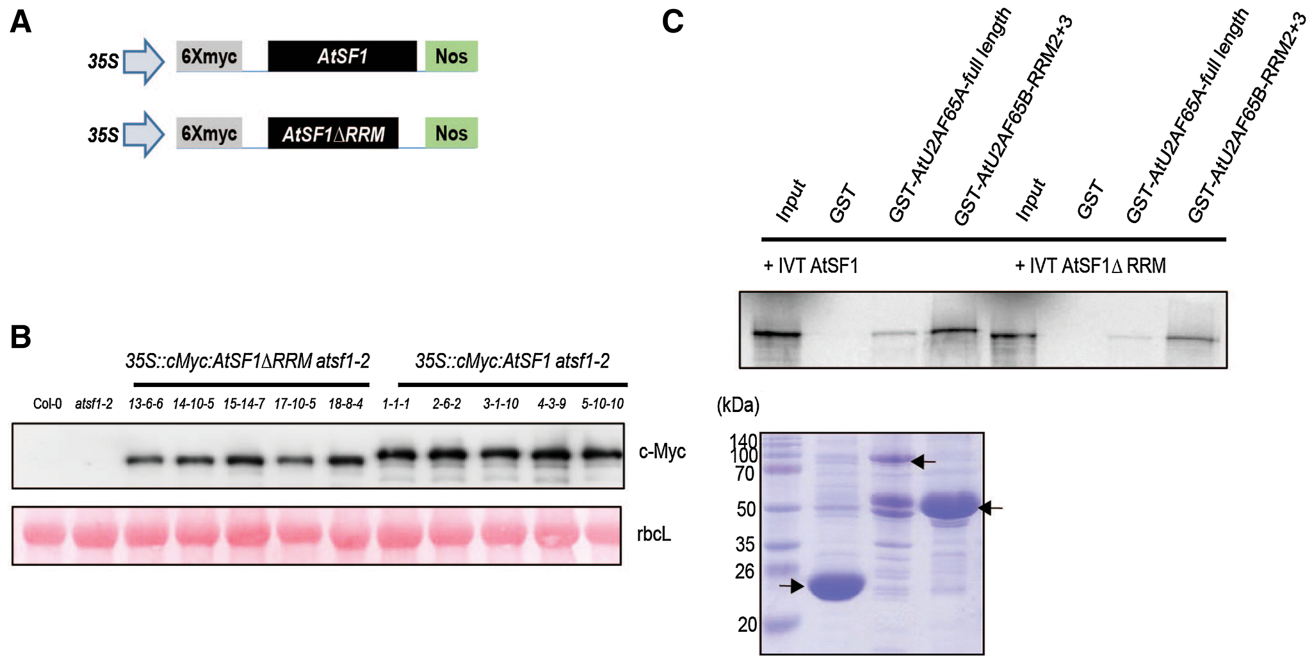

Fig. 1 Expression and binding affinity of AtSF1ΔRRM. **a** Schematic diagram of the transformation constructs used in this study. The *AtSF1* constructs with or without the RRM domain fused to the 6xcMyc tag at the N-terminus (*35S::cMyc:AtSF1* and *35S::cMyc:AtSF1ΔRRM*) were transformed into *atsf1-2* mutants. **b** Western blot analysis using anti-cMyc antibody. The recombinant cMyc-AtSF1 protein was detected in *35S::cMyc:AtSF1ΔRRM atsf1-2* and *35S::cMyc:AtSF1 atsf1-2* plants. Ponceau S-stained Rubisco large subunit (rbcL) was used as a loading control. **c** In vitro interaction between AtSF1ΔRRM and AtU2AF65 proteins. Full length of AtU2AF65a (RRM1/2/3) or truncated versions of AtU2AF65b (RRM2/3) proteins were fused to glutathione *S*-transferase (GST). GST or GST-tagged proteins were incubated with in vitro translated (IVT) AtSF1 proteins (*35S*-labeled). The *bands* indicate the eluted AtSF1 proteins visualized by autoradiography. The input lanes contain 10% of the *35S*-labeled proteins. Coomassie blue-stained bands indicated by *asterisks* show the amount and quality of the GST or GST fusion proteins used in this assay

atsf1-2 plants in the T_3 generation. As shown in Fig. 2b, Fig. S3A, and Supplementary Table S2, the respective *pAtSF1*$_{2.4kb}$*::AtSF1ΔRRM:GUS atsf1-2* plants partially rescued the early flowering phenotype of *atsf1-2* mutants, flowering at the approximately 13-leaf stage under LD conditions at 23 °C. Furthermore, the leaf size of *pAtSF1*$_{2.4kb}$*::AtSF1ΔRRM:GUS atsf1-2* plants was approximately 650 mm^2, smaller than in the wild-type plants, where it was approximately 820 mm^2 (Fig. 2c; Fig. S3B). Meanwhile, *pAtSF1*$_{2.4kb}$*::AtSF1 atsf1-2* plants used as a control completely complemented the effect of the *atsf1* mutation on flowering time and leaf size. However, the height of *pAtSF1*$_{2.4kb}$*::AtSF1ΔRRM:GUS atsf1-2*, *pAtSF1*$_{2.4kb}$*::AtSF1 atsf1-2*, and wild-type plants was the same (Fig. 2d). These results indicate that the expression of *AtSF1ΔRRM* under its own promoter only partially restores some of the developmental defects of *atsf1-2* mutants.

The deletion of conserved signature sequence motifs (RNP1 and RNP2) within the RRM domain is known to abolish the ability of the RRM domain to bind RNA (Burd and Dreyfuss 1994). Therefore, we also generated transgenic plants in which both RNP1 and RNP2 were deleted from AtSF1 (*pAtSF1*$_{964bp}$*::AtSF1ΔRNP1/2:GUS*) (Fig. 2a). We used the shorter version of the endogenous *AtSF1* promoter (964 bp), because it was also effective for this experiment (unpublished, Wang EJ, and Kim J-K) and was technically easier to work with when making the mutant AtSF1 constructs. In vivo production of recombinant proteins was confirmed by histochemical GUS staining of transgenic plants (Fig. S4A). Six independent *pAtSF1*$_{964bp}$*::AtSF1ΔRNP1/2:GUS atsf1-2* plants showed similar rescued phenotypes (Fig. 2e; Fig. S4B and C); these phenotypes were also observed in *pAtSF1*$_{2.4kb}$*::AtSF1ΔRRM:GUS atsf1-2* plants (Fig. 2b–d; Fig. S3, and Supplementary Table S2). Meanwhile, *pAtSF1*$_{964bp}$*::AtSF1:GUS atsf1-2* plants exhibited fully complemented phenotypes. This result indicates that, like *AtSF1ΔRRM,* the expression of *AtSF1ΔRNP1/2* also only partially recovers the effect of the *atsf1-2* mutation.

Taken together, these results suggest that the RRM domain of AtSF1 is important for the full function of the AtSF1 protein in plant development processes such as flowering time and plant size.

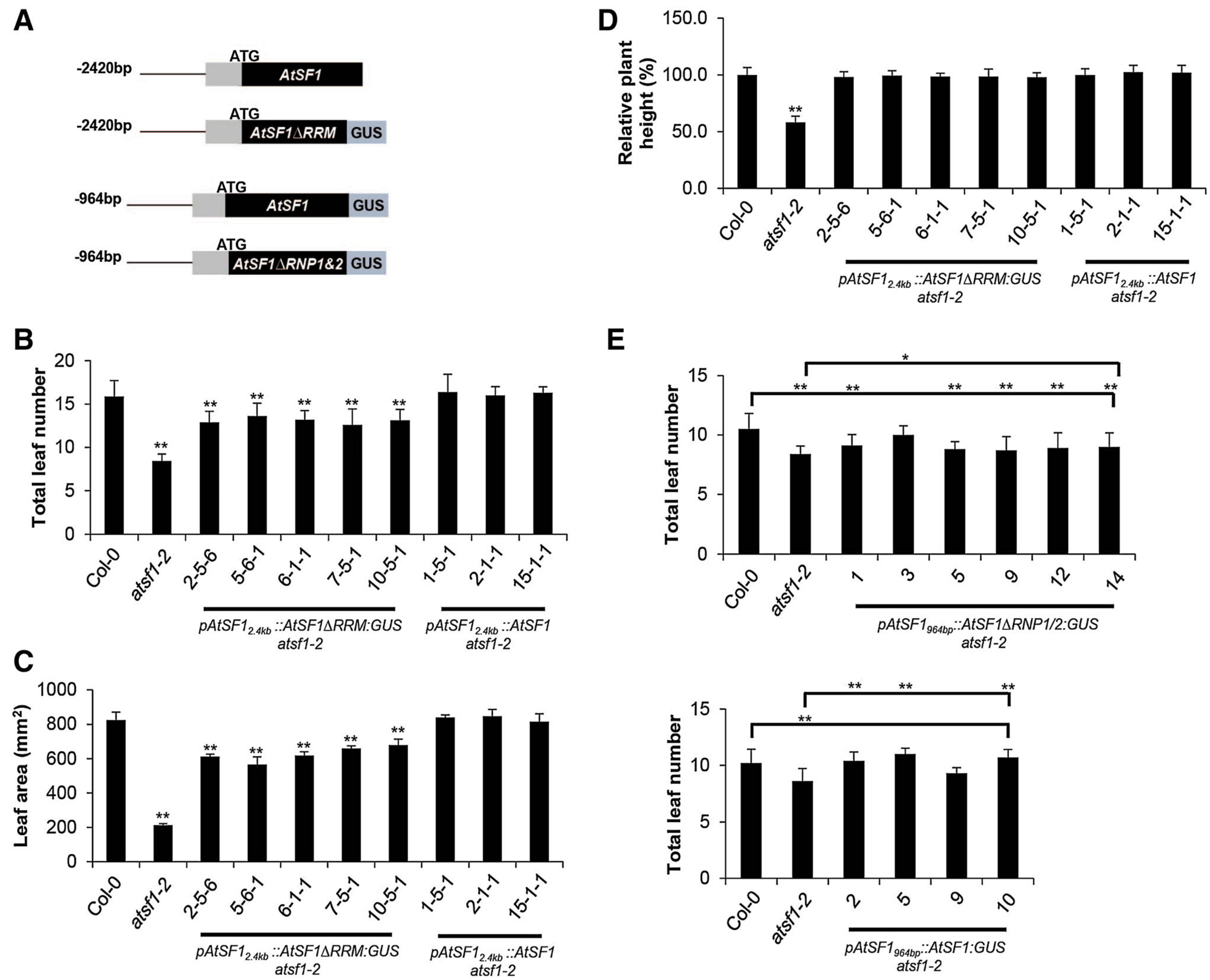

Fig. 2 Phenotypic analysis of *pAtSF1*$_{2.4kb}$*::AtSF1ΔRRM:GUS atsf1-2* and *pAtSF1*$_{964bp}$*::AtSF1ΔRNP1/2:GUS atsf1-2* plants. **a** Schematic diagram of the transformation constructs used in this study. The *AtSF1* constructs without the RRM domain (*pAtSF1*$_{2.4kb}$*::AtSF1ΔRRM:GUS*) or RNP1/2 (*pAtSF1*$_{964bp}$*::AtSF1ΔRNP1/2:GUS*) under its own promoter were transformed into *atsf1-2* mutants. **b** Flowering time, **c** leaf area, and **d** plant height of independent *pAtSF1*$_{2.4kb}$*::AtSF1ΔRRM:GUS atsf1-2* transgenic lines (T_3 generation) at 23 °C under long-day (LD) conditions. As a control, independent *pAtSF1*$_{2.4kb}$*::AtSF1 atsf1-2* transgenic lines were used. Rosette leaf area was analyzed using the ImageJ software. Error bars indicate the standard error of the mean (SEM) of three biological replicates. *Asterisks* indicate a significant difference in phenotypes of transgenic plants compared with those of wild-type (Col-0) plants (Student's *t* test, $*P < 0.05$, $**P < 0.01$). **e** Flowering time of independent *pAtSF1*$_{964bp}$*::AtSF1ΔRNP1/2:GUS atsf1-2* transgenic lines (T_2 generation) at 23 °C under LD conditions. As a control, independent *pAtSF1*$_{964bp}$*::AtSF1:GUS atsf1-2* transgenic lines were used. *Asterisks* indicate a significant difference in phenotype of transgenic plants compared with that of *atsf1-2* mutants (*upper bracket*) or wild-type plants (*lower bracket*) (Student's *t* test, $*P < 0.05$, $**P < 0.01$)

The RRM domain of AtSF1 affects alternative splicing of only specific subsets of transcripts like *FLM* pre-mRNA

To examine whether the partial restoration of flowering time seen in AtSF1 transgenic plants lacking the entire RRM domain or the RNP1/2 motifs correlated with changes in flowering time gene expression, we performed quantitative reverse transcription PCR (qRT-PCR) analysis of 8-day-old whole seedlings grown at 23 °C. *SHORT VEGETATIVE PHASE* (*SVP*) and *FLOWERING LOCUS M* (*FLM*) expression decreased significantly in *atsf1-2* mutants, whereas their expression in *pAtSF1*$_{964bp}$*::AtSF1ΔRNP1/2:GUS atsf1-2* plants was similar to their expression in *pAtSF1*$_{964bp}$*::AtSF1:GUS atsf1-2* and wild-type plants (Fig. 3a). RT-PCR analysis of *pAtSF1*$_{2.4kb}$*::AtSF1ΔRRM:GUS atsf1-2* plant also showed similar gene expression pattern (Fig. S6A). However, the expression levels of *FLOWERING LOCUS T* (*FT*) and *SUPPRESSOR OF OVEREXPRESSION OF CONSTANS1* (*SOC1*), which

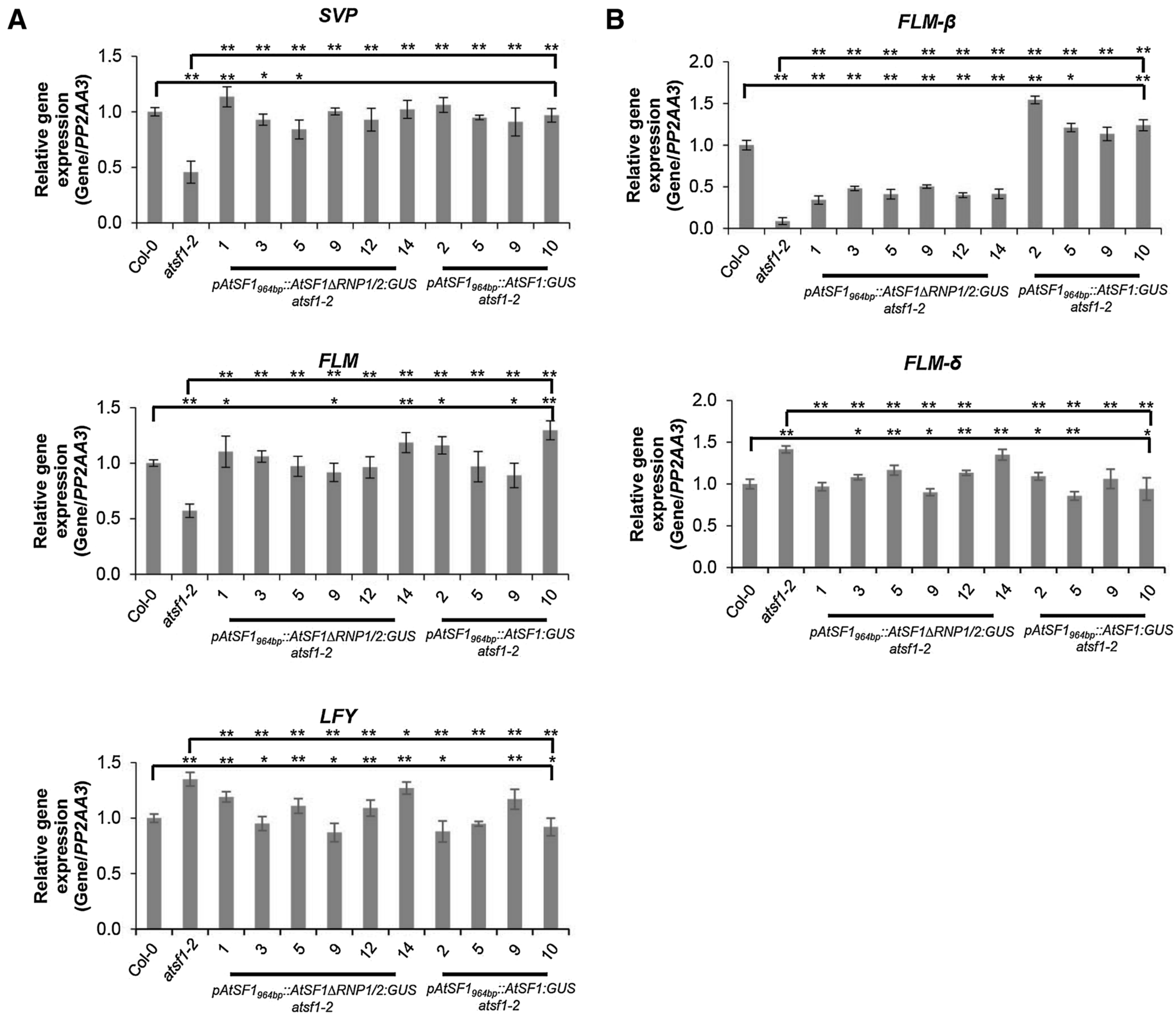

Fig. 3 Expression of flowering time genes in *pAtSF1*$_{964bp}$*::AtSF1ΔRNP1/2:GUS atsf1-2* plants. **a** *SVP*, *FLM,* and *LFY* expression in independent *pAtSF1*$_{964bp}$*::AtSF1ΔRNP1/2:GUS atsf1-2* lines grown at 23 °C under LD conditions. Total RNA was isolated from 8-day-old seedlings. As a control, independent *pAtSF1*$_{964bp}$*::AtSF1 atsf1-2* transgenic lines were used. The expression levels in wild-type plants were set to 1.0. *Error bars* indicate SEM of three biological replicates. *Asterisks* indicate a significant difference in the phenotype of transgenic plants compared with the *atsf1-2* mutants (*upper bracket*) or wild-type plants (*lower bracket*) (Student's *t* test, $^{*}P < 0.05$, $^{**}P < 0.01$). **b** Expression of two *FLM* splicing forms (*FLM-β* and *FLM-δ*) in independent *pAtSF1*$_{964bp}$*::AtSF1ΔRNP1/2:GUS atsf1-2* lines

are major downstream targets of *FLM* and *SVP* (Lee et al. 2013; Pose et al. 2013), were reduced in *atsf1-2* mutants, even though their expression was recovered in the rescued transgenic plants (Fig. S5). Because *FT* and *SOC1* expression could not explain the early flowering phenotype shown in the *atsf1-2* mutants (Fig. 2b, e; Fig. S2A, and Supplementary Table S2), we assessed the expression of downstream floral integrator genes such as *APETALA1* (*AP1*) and *LEAFY* (*LFY*). As shown in Fig. 3a, *LFY* expression was increased marginally in *atsf1-2* mutants, whereas its expression was similar or slightly higher in the rescued transgenic plants as compared with WT. However, *AP1* expression was nearly similar in all examined plants (Fig. S5). These results suggest that the altered expression levels of *FLM*, *SVP*, and *LFY* could explain the flowering phenotype of *atsf1-2* and the rescued transgenic plants.

We next investigated the expression levels of two *FLM* splicing forms (*FLM-β* and *FLM-δ*) in *atsf1-2*, *pAtSF1*$_{964bp}$*::AtSF1ΔRNP1/2:GUS atsf1-2,* and *pAtSF1*$_{2.4kb}$*::AtSF1ΔRRM:GUS atsf1-2* plants. In *atsf1-2* mutants, *FLM-β* transcript levels decreased, whereas those of *FLM-δ* marginally increased (Fig. 3b; Fig. S6B).

Interestingly, the level of *FLM-β* transcripts in *pAtSF1*$_{964bp}$*::AtSF1ΔRNP1/2:GUS atsf1-2* and *pAtSF1*$_{2.4kb}$*::AtSF1ΔRRM:GUS atsf1-2* plants increased only marginally when compared with *atsf1-2* mutants, whereas *FLM-δ* transcript levels in *pAtSF1*$_{964bp}$*::AtSF1ΔRNP1/2:GUS atsf1-2* and *pAtSF1*$_{2.4kb}$*::AtSF1ΔRRM:GUS atsf1-2* plants were similar to wild-type plants (Fig. 3b; Fig. S6B). This result suggests that the RRM domain of AtSF1 may affect the alternative splicing of *FLM* to produce the *FLM-β* splicing isoform.

Because splicing-defective mutants such as *protein arginine methyltransferase 5* (*prmt5*) and *spliceosomal timekeeper locus1* (*stip1*) globally affect the splicing patterns of circadian clock genes (Hong et al. 2010; Jones et al. 2012), we also examined alternative splicing isoforms of *LATE ELONGATED HYPOCOTYL* (*LHY*), *CIRCADIAN CLOCK ASSOCIATED1* (*CCA1*), and *TIMING OF CAB EXPRESSION1* (*TOC1*) in *pAtSF1*$_{2.4kb}$*::AtSF1ΔRRM:GUS atsf1-2* plants. As shown in Fig. S6C, the expression levels of major and minor spliced transcripts (arrows) of *LHY*, *CCA1*, and *TOC1* differed in *atsf1-2* mutants compared with wild-type plants. Conversely, the major or minor transcript levels of these genes were restored in *pAtSF1*$_{2.4kb}$*::AtSF1ΔRRM:GUS atsf1-2* and *pAtSF1*$_{2.4kb}$*::AtSF1 atsf1-2* plants, indicating that the deletion of the RRM domain in the AtSF1 does not affect alternative splicing of *LHY*, *CCA1*, and *TOC1*.

Taken together, these results suggest that the RRM domain of AtSF1 affects the alternative splicing of only specific subsets of transcripts.

Expression of AtSF1 lacking its RRM domain only marginally restores the hyposensitivity of *atsf1* mutants to heat stress

Our previous findings have shown that many heat shock protein-encoding genes are highly expressed in *atsf1-2* mutants at 23 °C under LD conditions (Jang et al. 2014). Therefore, to examine whether *AtSF1* is involved in modulating the heat stress response, we first tested the heat stress response of *atsf1-2* mutants. Under heat stress conditions (45 °C, 70 min), *atsf1-2* mutants exhibited increased resistance to heat (78% survival rate), whereas wild-type plants did not (55% survival rate) (Fig. 4a, b), suggesting that the *AtSF1* functions as a negative regulator of the heat stress response. Under the same conditions, *35S::FCA* and *fca-9* plants as controls showed increased and reduced resistance to heat, respectively (Fig. 4a, c) (Lee et al. 2015).

As the *AtSF1* and *FCA* mutant plants have opposite responses to heat stress conditions (Fig. 4) and *AtSF1* affects alternative splicing of some pre-mRNAs (Jang et al. 2014), we investigated the expression levels of alternatively spliced *FCA* transcripts. RT-PCR data revealed that the expression levels of *FCA- γ*, *FCA-β*, and *FCA-α* were not significantly altered in *atsf1-2* mutants compared with wild-type plants (Fig. S7). This result suggests that the increased tolerance of *atsf1-2* mutants to heat stress is not associated with the alternative splicing patterns of *FCA*.

To investigate whether the RRM domain of AtSF1 affects the response of *atsf1-2* mutants to heat stress, we next treated *pAtSF1*$_{2.4kb}$*::AtSF1ΔRRM:GUS atsf1-2* plants at 45 °C for 70 min. *pAtSF1*$_{2.4kb}$*::AtSF1ΔRRM:GUS atsf1-2* plants showed increased resistance to heat, with a comparable survival rate to the *atsf1-2* mutants (71% surviving) (Fig. 4a, b). Meanwhile, *pAtSF1*$_{2.4kb}$*::AtSF1 atsf1-2* showed a similar heat response to that of wild-type plants (59% survival rate). This result suggests that the expression of *AtSF1ΔRRM* suppresses the thermotolerance shown in *atsf1-2* mutants only marginally, if at all.

The transcript levels of a heat shock transcription factor (*HsfA2*, *AT2G26150*) and five heat shock genes that are direct downstream targets of *HsfA2* were up-regulated in the *atsf1-2* mutant under non-heat stress conditions (Jang et al. 2014). In addition, after heat stress treatment (45 °C for 70 min), the differences in *HsfA2* expression between wild-type and *atsf1-2* mutants were nearly identical (Fig. S8). Thus, we examined the expression levels of *HsfA2* and seven heat shock genes in *pAtSF1*$_{964bp}$*::AtSF1ΔRNP1/2:GUS atsf1-2* plants grown at 23 °C under LD conditions. Two *HSFA2* transcripts (*HsfA2* and *HsfA2-II*) in wild-type plants were detected, whereas only *HsfA2* transcripts known as a functional form of *HsfA2* were detected in *atsf1-2* mutants (Fig. 5; Fig. S8). In addition, the expression levels of direct targets of *HsfA2* were higher in *atsf1-2* mutants than those in wild-type plants under the same conditions. These results suggest that already enhanced accumulation of these heat shock response genes may be responsible for increased resistance to heat treatments in *atsf1-2* mutants (Fig. 4).

Consistent with the partially rescued phenotype of *pAtSF1*$_{2.4kb}$*::AtSF1 atsf1-2* transgenic plants under heat stress conditions (Fig. 4), RT-PCR data showed that the expression levels of *HsfA2*, *AT4G10250, AT5G12030*, *AT1G52560*, *AT5G37670*, and *AT1G53540* were nearly restored to wild-type levels, whereas the expression levels of *AT5G12020* and *AT4G25200* were not (Fig. 5b). Of the seven heat shock genes examined, only *AT5G12020* and *AT4G25200* are not direct targets of *HsfA2* (Nishizawa et al. 2006), potentially accounting for their unaltered expression patterns in transgenic plants. Interestingly, alternatively spliced *HsfA2* transcripts (*HSFA2-II*) as a signature of the cytosolic protein response in *Arabidopsis* (Sugio et al. 2009) were still detected in *pAtSF1*$_{964bp}$*::AtSF1ΔRNP1/2:GUS atsf1-2* plants (Fig. 5a, b), suggesting

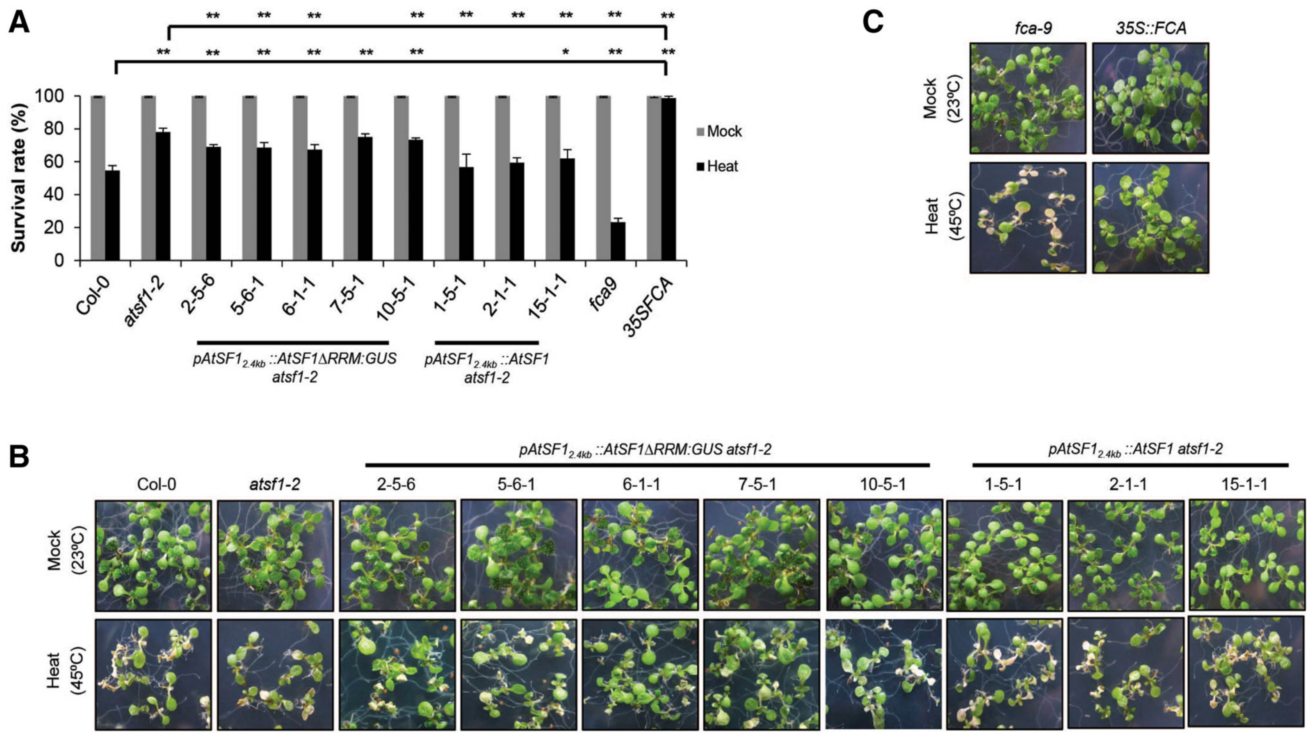

Fig. 4 Response of *pAtSF1*$_{2.4kb}$*::AtSF1ΔRRM:GUS atsf1-2* plants to heat stress treatments. **a** Survival rate and **b**, **c** photographs of 1-week-old transgenic plants under heat stress conditions. The plants grown on MS plates were exposed to heat (45 °C for 70 min) and allowed to recover at 23 °C for 3 days. As a control, independent *pAtSF1*$_{2.4kb}$*::AtSF1 atsf1-2* transgenic lines were used. The phenotypes of *35S::FCA* and *fca-9* in response to heat stress were consistent with a previous report (Lee et al. 2015). Survival rates of three biological replicates were measured. *Asterisks* indicate a significant differences in the response of transgenic plants compared with *atsf1-2* mutants (*upper bracket*) or wild-type plants (*lower bracket*) (Student's *t* test, $*P < 0.05$, $**P < 0.01$). *Error bars* indicate SEM of three biological replicates

that the RRM domain may affect exon-skipping type alternative splicing.

Taken together, these results suggest that the partially rescued heat response shown in *pAtSF1*$_{2.4kb}$*::AtSF1ΔRRM:GUS atsf1-2* plants is correlated with the expression of *HsfA2* and five *HsfA2* target genes.

Discussion

AtSF1 contains at least three domains (a KH, a zinc finger, and an RRM); while the conserved domains, like the KH domain, are expected to have similar functions to their counterparts in yeast and metazoan, little research has been conducted on the role of these structural domains. In this study, we provide evidence that AtSF1 functions in the control of flowering time and the heat stress response and that the RRM domain is important for AtSF1 activity in these processes.

We have recently reported that a mutation in *AtSF1* leads to slightly early flowering (Jang et al. 2014). Furthermore, several studies have revealed that misexpression of some splicing factors such as *serine-arginine 45* (*SR45*) and *PROTEIN ARGININE METHYL TRANSFERASE 5* (*PRMT5*)/*Shk1 kinase binding protein1* (*SKB1*) alters flowering time (Ali et al. 2007; Zhang et al. 2011). Based on complementation studies and expression analyses (Figs. 2, 3; Figs. S2, S3, and S5, and Supplementary Table S2), we have here shown that the early flowering phenotype of *atsf1-2* mutants was associated with up-regulation of *LFY*, and down-regulation of *FLM* and *SVP*. Our results suggest that AtSF1 may control flowering time by regulating *LFY* expression through an *FLM* and *SVP*-dependent pathway. This is consistent with evidence showing that the flowering time of *35S::LFY fve-1* plants was similar to that of *35S::LFY* plants (Nilsson et al. 1998), that *svp-32 fca-9* or *svp-32 fve-3* plants flowered with similar leaf numbers as *svp-32* plants (Lee et al. 2007), and that *svp-32 flm-3* plants have additive flowering time (Lee et al. 2013). In addition, altered activity in other E′ complex components such as AtU2AF35a or AtU2AF35b results in altered flowering time (Wang and Brendel 2006). Thus, it is probable that AtSF1 regulates the expression of a subset of flowering time genes and thereby modulates flowering time.

Notably, reduced expression levels of *FLM-β,* but not *FLM-δ,* were observed in *atsf1-2* mutants (Fig. 3b;

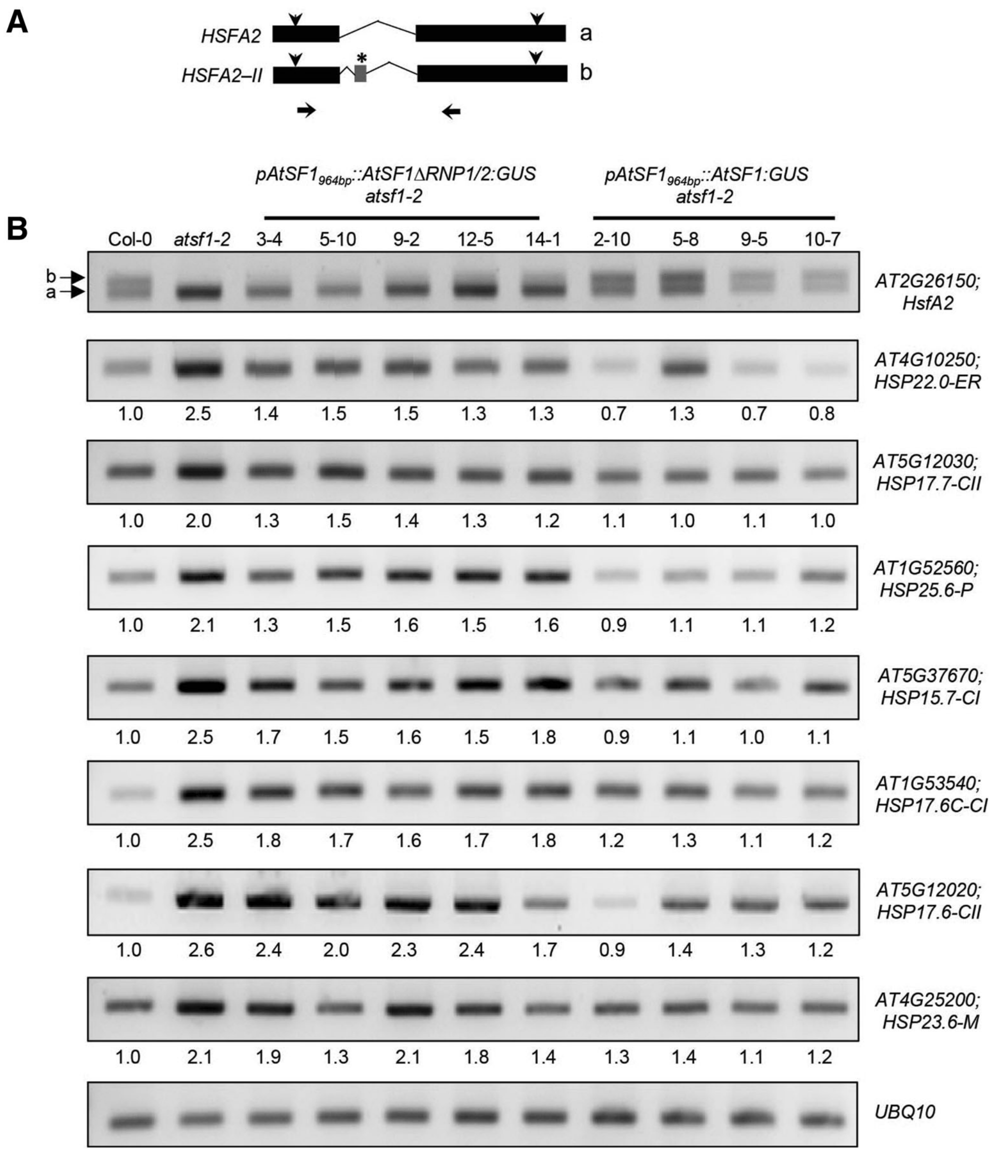

Fig. 5 Expression of heat stress-related genes in *pAtSF1*$_{964bp}$*::AtSF1ΔRNP1/2:GUS atsf1-2* plants. **a** Schematic diagrams of two spliced variants (*HSFA2* and *HSFA2-II*) of *HsfA2*. The letters '*a*' and '*b*' adjacent to the gel image indicate *HSFA2* and *HSFA2-II*, respectively. The *black boxes*, *gray box*, and *lines* indicate the exons, alternative exon, and introns, respectively. The *arrowheads* above the exons indicate the start and stop codons, respectively. The *black arrows* below the gene structure indicate the positions of the forward and reverse primers. **b** Expression of *HsfA2* and seven *HSP* gene expressions in independent *pAtSF1*$_{964bp}$*::AtSF1ΔRNP1/2:GUS atsf1-2* lines grown at 23 °C under LD conditions. Total RNA was isolated from 8-day-old seedlings. As a control, independent *pAtSF1*$_{964bp}$*::AtSF1 atsf1-2* transgenic lines were used. The *numbers* below the gel panels represent the average band intensities of three biological replicates. The signal in wild-type plants was set to 1.0. The band intensity was analyzed using the Quantity One program (Biorad). *UBQ10* gene was used as an internal control

Fig. S6B), suggesting that AtSF1 could affect alternative splicing of *FLM* pre-mRNA to produce *FLM-β* transcripts. The early flowering phenotype of *flm-3* mutants (Lee et al. 2013; Pose et al. 2013) is consistent with the phenotype of *atsf1-2* mutants (Fig. 2; Fig. S2, and Supplementary Table S2). Our evidence that *pAtSF1*$_{964bp}$*:: AtSF1ΔRNP1/2:GUS atsf1-2* and *pAtSF1*$_{2.4kb}$*::AtSF1ΔRRM:GUS atsf1-2* plants had reduced *FLM-β* expression (Fig. 3b; Fig. S6B) could explain why *pAtSF1*$_{964bp}$*:: AtSF1ΔRNP1/2:GUS atsf1-2* or *pAtSF1*$_{2.4kb}$*::AtSF1ΔRRM:GUS atsf1-2* plants could partially recover the effect of the *atsf1-2* mutation on flowering time (Fig. 2; Supplementary Table S2). This result implies that the RRM domain of AtSF1 affects the alternative splicing of *FLM* to produce the alternatively spliced *FLM-β* isoform. The temperature-dependent alternative splicing of *FLM* produces antagonistic *FLM-β* and *FLM-δ* isoforms that affect ambient temperature-responsive flowering (Pose et al. 2013). Moreover, loss of *AtSF1* activity leads to temperature-insensitive flowering phenotype (unpublished, Lee KC, Lee JH, and Kim J-K). Thus, the analysis of the flowering phenotype of the transgenic plants in which the RRM domain of *AtSF1* is absent at different temperatures, and *FLM-β* and *FLM-δ* expression in *atsf1-2* mutant at different temperatures will clarify the role of *AtSF1* in ambient temperature-responsive flowering.

A recent report has shown that alternative splicing coupled with nonsense-mediated mRNA decay (AS-NMD) modulates *FLM*-mediated thermal induction of flowering (Sureshkumar et al. 2016). Moreover, alteration of *AtSF1* function affects the patterns of alternative splicing of some specific transcripts, which produces aberrantly spliced transcripts (Jang et al. 2014). These results suggest that alternative splicing of *FLM* pre-mRNA by AtSF1 may interconnect with AS-NMD regulatory mechanism in the regulation of ambient temperature-responsive flowering. This hypothesis is supported by our observation that *atsf1-2* mutants did not respond to changes in ambient temperature, as shown in *upframeshift* (*upf*) mutants (Sureshkumar et al. 2016). Furthermore, we observed non-canonical *FLM* transcripts produced from exon-skipping and intron retention events in *atsf1-2* mutants (unpublished, Lee KC, Lee JH, and Kim J-K). Thus, further investigation is required to elucidate the regulatory mechanism of alternative splicing of *FLM* pre-mRNA through interaction between *UPF* and *AtSF1* in the ambient temperature-responsive flowering.

Leaf size and plant height are two important growth traits regulated by a variety of environmental and genetic factors. In this study, our data showed that *atsf1* mutation resulted in the reduction of leaf size and plant height in *atsf1-2* mutant (Fig. 2c, d; Fig. S2B and C, Fig. S3, and Fig. S4B and C). In addition, several studies have revealed that leaf size is determined by interconnection between cell division and expansion in *Arabidopsis* (Gonzalez et al. 2012; Gonzalez and Inzé 2015). Furthermore, plant height is associated with stem elongation mediated by multiple phytohormones including gibberellin (GA), brassinosteroid (BR), and auxin (Wang and Li 2008). It raises the possibility that *AtSF1* may control leaf size and plant height by regulating a variety of genes. This notion is supported by our previous microarray data in *atsf1-2* mutant (Jang et al. 2014) that down-regulation of the genes involved in cell expansion such as *GROWTH-REGULATING FACTOR5* (*GRF5*), *AINTEGUMENTA* (*ANT*), and *TARGET OF RAPAMYCIN* (*TOR*) (Vanhaeren et al. 2014), and down-regulation of BR signaling pathway genes such as *BRASSINOSTEROID-INSENSITIVE 2* (*BIN2*) and *BRASSINAZOLE-RESISTANT 1* (*BZR1*) (Zhao et al. 2002; Wang et al. 2002). Moreover, we showed that *pAtSF1*$_{2.4kb}$*::AtSF1ΔRRM:GUS atsf1-2* plants did not fully recover the effect of the *atsf1* mutation on leaf size, but not plant height (Fig. 2c, d; Fig. S2B and C, Fig. S3, and Fig. S4B and C), suggesting that the RRM domain in AtSF1 may play a role in the leaf development.

Heat shock transcription factors are known to be the key players mediating plant responses to highly elevated temperature or under heat shock conditions (von Koskull-Döring et al. 2007). We have recently revealed that mutation of *AtSF1* results in the up-regulation of *HsfA2* and five heat shock genes that are direct downstream targets of *HsfA2* (Jang et al. 2014). These results imply that AtSF1 may mediate the heat response. Consistent with this hypothesis, the results of the current study showed that *atsf1-2* mutants exhibited increased tolerance to heat stress, whereas *pAtSF1*$_{2.4kb}$*::AtSF1 atsf1-2* plants showed reduced resistance to heat (Fig. 4). In addition, a functional form of *HsfA2* transcripts was significantly increased in *atsf1-2* mutants under non heat-stress conditions (Fig. 5; Fig. S8). Moreover, we showed that *pAtSF1*$_{2.4kb}$*::AtSF1ΔRRM:GUS atsf1-2* plants did not fully suppress the thermotolerance shown in *atsf1-2* mutants (Fig. 4), suggesting that the RRM domain in AtSF1 may play a role in the heat stress response. Give that the fact that several heat stress conditions affect alternative splicing of *HsfA2*, thereby differentially producing alternatively spliced *HsfA2* isoforms (*HsfA2-II* and *HsfA2-III*) (Sugio et al. 2009; Liu et al. 2013), it is expected that *AtSF1* is necessary for the alternative splicing of *HsfA2* pre-mRNA under a variety of heat stress conditions. Thus, it will be informative to determine whether *AtSF1* functions in wider heat stress treatments by the regulation of alternative splicing of *HsfA2*.

AtSF1 as a splicing factor negatively regulates heat stress (Fig. 4) and the overexpression of *FCA*, which is known to produce four different spliced transcripts (Macknight et al. 2002), causes resistant to heat stress (Lee et al. 2015); an important question is, therefore, whether AtSF1 controls thermotolerance by directly modulating the alternative splicing of *FCA*. The expression levels of three major *FCA* spliced isoforms were not significantly altered in *atsf1-2* mutants (Fig. S7), however, suggesting that AtSF1 may require downstream genes other than *FCA* for the regulation of the heat stress response. Further investigation into the downstream targets of AtSF1 will provide a better understanding of the modulation of thermotolerance by AtSF1.

If the RRM domain were essential for AtSF1 function, it would be expected that all the phenotypes of *atsf1-2* mutants would be restored in *pAtSF1*$_{2.4kb}$*::AtSF1ΔRRM:GUS atsf1-2* plants. However, *pAtSF1*$_{2.4kb}$*::AtSF1ΔRRM:GUS atsf1-2* plants completely complemented the ABA hypersensitivity shown in *atsf1-2* mutants, similar to *pAtSF1*$_{2.4kb}$*::AtSF1 atsf1-2* plants (Fig. S9). Moreover, the reduced expression of CYP707A2, which may be correlated with the ABA-hypersensitive phenotype of the *atsf1-2* mutants, was fully recovered in *pAtSF1$_{964bp}$::AtSF1ΔRNP1/2:GUS atsf1-2* plants (Fig. S10); this is an apparent inconsistency with other phenotypes observed in *pAtSF1$_{2.4kb}$::AtSF1ΔRRM:GUS atsf1-2* plants (Figs. 2, 4; Figs. S2, S3, S4). These results suggest that AtSF1 protein lacking the RRM domain still has sufficient activity for pre-mRNA splicing of genes important for the ABA response.

The RRM domain functions not only as an RNA-binding motif but also a protein–protein interaction motif (Rain et al. 1998; Thickman et al. 2006; Loerch and Kielkopf 2016). For example, the RRM domain of the yeast U2AF23 (human U2AF35 counterpart) protein works as a frame, such that two zinc finger domains of yeast U2AF23 are arranged side by side on the RRM to bind the 3′ splice site of pre-mRNA (Yoshida et al. 2015).

Further study will provide new insight into the role of the RRM domain of AtSF1 in plant-specific pre-mRNA splicing processes.

Author contribution statement J-KK conceived and designed the research. KCL conducted experiments. KCL, YHJ, S-KK, H-YP, MPT, JHL, and J-KK analyzed data. KCL, JHL, and J-KK wrote the manuscript. All authors read and approved the manuscript.

Acknowledgements This work was supported by the Basic Science Research Program through the National Research Foundation of Korea funded by the Ministry of Education (2014R1A1A2055796 to J.-K. Kim) and a Korea University Grant (to J.-K. Kim).

Compliance with ethical standards

Conflict of interest The authors have no conflicts of interest to declare.

References

Abovich N, Rosbash M (1997) Cross-intron bridging interactions in the yeast commitment complex are conserved in mammals. Cell 89:403–412

Adam SA, Nakagawa T, Swanson MS, Woodruff TK, Dreyfuss G (1986) mRNA polyadenylate-binding protein: gene isolation and sequencing and identification of a ribonucleoprotein consensus sequence. Mol Cell Biol 6:2932–2943

Alba MM, Pages M (1998) Plant proteins containing the RNA-recognition motif. Trends Plant Sci 3:15–21

Ali GS, Palusa SG, Golovkin M, Prasad J, Manley JL, Reddy AS (2007) Regulation of plant developmental processes by a novel splicing factor. PLoS One 2:e471

Arning S, Gruter P, Bilbe G, Kramer A (1996) Mammalian splicing factor SF1 is encoded by variant cDNAs and binds to RNA. RNA 2:794–810

Bentley RC, Keene JD (1991) Recognition of U1 and U2 small nuclear RNAs can be altered by a 5-amino-acid segment in the U2 small nuclear ribonucleoprotein particle (snRNP) B″ protein and through interactions with U2 snRNP-A′ protein. Mol Cell Biol 11:1829–1839

Berglund JA, Chua K, Abovich N, Reed R, Rosbash M (1997) The splicing factor BBP interacts specifically with the pre-mRNA branchpoint sequence UACUAAC. Cell 89:781–787

Berglund JA, Fleming ML, Rosbash M (1998) The KH domain of the branchpoint sequence binding protein determines specificity for the pre-mRNA branchpoint sequence. RNA 4:998–1006

Birney E, Kumar S, Krainer AR (1993) Analysis of the RNA-recognition motif and RS and RGG domains: conservation in metazoan pre-mRNA splicing factors. Nucleic Acids Res 21(25):5803–5816

Burd CG, Dreyfuss G (1994) Conserved structures and diversity of functions of RNA-binding proteins. Science 265:615–621

Chen M, Manley JL (2009) Mechanisms of alternative splicing regulation: insights from molecular and genomics approaches. Nat Rev Mol Cell Biol 10(11):741–754

Chen R, Silver DL, de Bruijin FJ (1998) Nodule parenchyma-specific expression of the *Sesbania rostrata* early nodulin gene SrEnod2 is mediated by its 3′ untranslated region. Plant Cell 10:1585–1602

Fujii H, Chinnusamy V, Rodrigues A, Rubio S, Antoni R, Park SY et al (2009) In vitro reconstitution of an abscisic acid signalling pathway. Nature 462(3):660–664

Garrey SM, Voelker R, Berglund JA (2006) An extended RNA binding site for the yeast branch point-binding protein and the role of its zinc knuckle domains in RNA binding. J Biol Chem 281:27443–27453

Glisovic T, Bachorik JL, Yong J, Dreyfuss G (2008) RNA-binding proteins and posttranscriptional gene regulation. FEBS Lett 582:1977–1986

Gonzalez N, Inzé D (2015) Molecular systems governing leaf growth: from genes to networks. J Exp Bot 66(4):1045–1054

Gonzalez N, Vanhaeren H, Inzé D (2012) Leaf size control: complex coordination of cell division and expansion. Trends Plant Sci 17:332–340

Hong S, Song HR, Lutz K, Kerstetter RA, Michael TP, McClung CR (2010) Type II protein arginine methyltransferase 5 (PRMT5) is required for circadian period determination in *Arabidopsis thaliana*. Proc Natl Acad Sci USA 107:21211–21216

Jacewicz A, Chico L, Smith P, Schwer B, Shuman S (2015) Structural basis for recognition of intron branchpoint RNA by yeast Msl5 and selective effects of interfacial mutations on splicing of yeast pre-mRNAs. RNA 21:401–414

Jang YH, Park HY, Lee KC, May PT, Kim SK, Suh MC et al (2014) A homolog of splicing factor SF1 is essential for development and is involved in the alternative splicing of pre-mRNA in *Arabidopsis thaliana*. Plant J 78:591–603

Jones MA, Williams BA, McNicol J, Simpson CG, Brown JW, Harmer SL (2012) Mutation of *Arabidopsis* spliceosomal timekeeper locus1 causes circadian clock defects. Plant Cell 24:4066–4082

Jurica MS, Moore MJ (2003) Pre-mRNA splicing: awash in a sea of proteins. Mol Cell 12:5–14

Kim SK, Yun CH, Lee JH, Jang YH, Park HY, Kim JK (2008) *OsCO3*, a *CONSTANS-LIKE* gene, controls flowering by negatively regulating the expression of *FT*-like genes under SD conditions in rice. Planta 228:355

Lee JH, Yoo SJ, Park SH, Hwang I, Lee JS, Ahn JH (2007) Role of *SVP* in the control of flowering time by ambient temperature in *Arabidopsis*. Genes Dev 21(4):397–402

Lee JH, Ryu HS, Chung KS, Pose D, Kim SK, Schmid M et al (2013) Regulation of temperature-responsive flowering by MADS-box transcription factor repressors. Science 342(6158):628–632

Lee S, Lee HJ, Jung JH, Park CM (2015) The *Arabidopsis thaliana* RNA-binding protein FCA regulates thermotolerance by modulating the detoxification of reactive oxygen species. New Phytol 205:555–569

Liu Z, Luyten I, Bottomley M, Messias A, Houngninou-Molango S, Sprangers R et al (2001) Structural basis for recognition of the intron branch site by splicing factor 1. Science 294:1098–1102

Liu J, Sun N, Liu M, Liu J, Du B, Wang X et al (2013) An autoregulatory loop controlling *Arabidopsis* HsfA2 expression: role of heat shock-induced alternative splicing. Plant Physiol 162:512–521

Loerch S, Kielkopf CL (2016) Unmasking the U2AF homology motif family: a bona fide protein-protein interaction motif in disguise. RNA 22:1795–1807

Lorković ZJ (2009) Role of plant RNA-binding proteins in development, stress response and genome organization. Trends Plant Sci 14:229–236

Lorkvić ZJ, Barta A (2002) Genome analysis: RNA recognition motif (RRM) and K homology (KH) domain RNA binding proteins from the flowering plant *Arabidopsis thaliana*. Nucleic Acids Res 30(3):623–635

Lorković ZJ, Kirk DAW, Lambermon MHL, Filipowicz W (2000) Pre-mRNA splicing in higher plants. Trends Plant Sci 5:160–167

Macknight R, Duroux M, Laurie R, Dijkwel P, Simpson G, Dean C (2002) Functional significance of the alternative transcript processing of the *Arabidopsis* floral promoter FCA. Plant Cell 14:877–888

Maris C, Dominguez C, Allain FH (2005) The RNA recognition motif, a plastic RNA-binding platform to regulate post-transcriptional gene expression. FEBS J 272(9):2118–2131

Nilsson O, Lee I, Blazquez MA, Weigel D (1998) Flowering-time genes modulate the response to LEAFY activity. Genetics 150:403–410

Nishizawa A, Yabuta Y, Yoshida E, Maruta T, Yoshimura K, Shigeoka S (2006) *Arabidopsis* heat shock transcription factor A2 as a key regulator in response to several types of environmental stress. Plant J 48:535–547

Pose D, Verhage L, Ott F, Yant L, Mathieu J, Angenent GC et al (2013) Temperature-dependent regulation of flowering by antagonistic FLM variants. Nature 503:414–417

Rain JC, Rafi Z, Rhani Z, Legrain P, Kramer A (1998) Conservation of functional domains involved in RNA binding and protein–protein interactions in human and *Saccharomyces cerevisiae* pre-mRNA splicing factor SF1. RNA 4:551–565

Rutz B, Séraphin B (2000) A dual role for BBP/ScSF1 in nuclear pre-mRNA retention and splicing. EMBO J 19:1873–1886

Sachs AB, Bond MW, Kornberg RD (1986) A single gene from yeast for both nuclear and cytoplasmic polyadenylate-binding proteins: domain structure and expression. Cell 45:827–835

Schwartz SH, Silva J, Burstein D, Pupko T, Eyras E, Ast G (2008) Large-scale comparative analysis of splicing signals and their corresponding splicing factors in eukaryotes. Genome Res 18:88–103

Selenko P, Gregorovic G, Sprangers R, Stier G, Rhani Z, Kramer A et al (2003) Structural basis for the molecular recognition between human splicing factors $U2AF^{65}$ and SF1/mBBP. Mol Cell 11:965–976

Severing EI, Van Dijk ADJ, Morabito G, Busscher-Lange J, Immink RGH, Van Ham RCHJ (2012) Predicting the impact of alternative splicing on plant MADS domain protein function. PLoS One 7:e30524

Shitashige M, Satow R, Honda K, Ono M, Hirohashi S, Yamada T (2007) Increased susceptibility of $Sf1^{+/-}$ mice to azoxymethane-induced colon tumorigenesis. Cancer Sci 98:1862–1867

Sugio A, Dreos R, Aparicio F, Maule A (2009) The cytosolic protein response as a subcomponent of the wider heat shock response in *Arabidopsis*. Plant Cell 21:642–654

Sureshkumar S, Dent C, Seleznev A, Tasset C, Balasubramanian S (2016) Nonsense-mediated mRNA decay modulates FLM-dependent thermosensory flowering response in *Arabidopsis*. Nat Plants 29:16055

Tanackovic G, Krämer A (2005) Human splicing factor SF3a, but not SF1, is essential for pre-mRNA splicing in vivo. Mol Biol Cell 16:1366–1377

Tao S, Arnaud G, Ludovic G, Kamel H, Alice B, Maureen RH et al (2013) An RNA recognition motif-containing protein is required for plastid RNA editing in *Arabidopsis* and maize. Proc Natl Acad Sci USA 110(12):E1169–E1178

Thickman KR, Swenson MC, Kabogo JM, Gryczynski Z, Kielkopf CL (2006) Multiple U2AF65 binding sites within SF3b155: thermodynamic and spectroscopic characterization of protein–protein interactions among pre-mRNA splicing factors. J Mol Biol 356:664–683

Vanhaeren H, Gonzalez N, Coppens F, De Milde L, Van Daele T, Vermeersch M et al (2014) Combining growth-promoting genes leads to positive epistasis in *Arabidopsis thaliana*. eLife 3:e02252

Von Koskull-Döring, Scharf KD, Lutz Nover (2007) The diversity of plant heat stress transcription factors. Trends Plant Sci 12(10):1360–1385

Wang BB, Brendel V (2006) Genome wide comparative analysis of alternative splicing in plants. Proc Natl Acad Sci USA 103:7175–7180

Wang Y, Li J (2008) Molecular basis of plant architecture. Annu Rev Plant Biol 59:253–279

Wang ZY, Nakano T, Gendron J, He J, Chen M, Vafeados D et al (2002) Nuclear-localized BZR1 mediates brassinosteroid-induced growth and feedback suppression of brassinosteroid biosynthesis. Dev Cell 2:505–513

Webb CJ, Lakhe-Reddy S, Romfo CM, Wise JA (2005) Analysis of mutant phenotypes and splicing defects demonstrates functional collaboration between the large and small subunits of the essential splicing factor U2AF in vivo. Mol Biol Cell 16(2):584–596

Weigel D, Glazebrook J (2006) In planta transformation of *Arabidopsis*. Cold Spring Harb Protoc. doi:10.1101/pdb.prot4668

Will CL, Luhrmann R (2011) Spliceosome structure and function. Cold Spring Harbor Perspect Biol 3:a003707

Yoshida H, Park SY, Akiyoshi T, Sato M, Shirouzu M, Tsuda K, Kuwasako K, Unzai S, Muto Y, Urano T, Obayashi E (2015) A novel 3'splice site recognition by the two zinc fingers in the U2AF small subunit. Genes Dev 29(15):1649–1660

Zhang Z, Zhang S, Zhang Y, Wang X, Li D, Li Q et al (2011) *Arabidopsis* floral initiator SKB1 confers high salt tolerance by regulating transcription and pre-mRNA splicing through altering histone H4R3 and small nuclear ribonucleoprotein LSM4 methylation. Plant Cell 23:396–411

Zhao J, Peng P, Schmitz RJ, Decker AD, Tax FE, Li J (2002) Two putative BIN2 substrates are nuclear components of brassinosteroid signaling. Plant Physiol 130:1221–1229